Highly birefringent liquid-crystalline polymers for photonic applications: synthesis of liquid-crystalline polymers with side-chain azo-tolane mesogens and their holographic properties

Kunihiko Okano, Atsushi Shishido, Osamu Tsutsumi,† Takeshi Shiono‡ and Tomiki Ikeda*

Received 3rd May 2005, Accepted 24th June 2005
First published as an Advance Article on the web 12th July 2005
DOI: 10.1039/b506131h

We have synthesized highly birefringent liquid-crystalline polymers (LCPs) containing an azobenzene group directly connected to a tolane moiety (**P3AT*m***), in which the alkyl spacer length $(CH_2)_m$ was varied as $m = 6$, 9 and 12. All LCPs showed a nematic phase in a broad temperature range (>170 °C). The homogeneously aligned LCP films showed a high value of birefringence (about 0.4) and a large change in the birefringence could be induced by photoinduced alignment change. Grating formation of LCPs has been explored in a glassy state. The diffraction efficiency (η) showed a maximum when an order–disorder change was completed in the bright areas of the interference patterns. Studies on the effects of light intensity on the grating formation suggested that the diffraction efficiency was high ($\eta = 20\%$) even though the alignment change of the azo-tolane moieties was small. Furthermore, the behavior of the grating formation was found to be dependent on the alkyl spacer length of **P3AT*m***.

Introduction

Recently, the demand for higher storage capacity in optical data storage is rapidly increasing, and holographic technology has been applied for data storage, display, and optical elements, because the information packing densities can be increased drastically by using 3-D storage techniques. In holography, diffraction efficiency (η) is one of the most important factors to evaluate the ability of the materials. The diffraction efficiency of phase-type gratings is higher than that of amplitude-type ones because the former are formed by a change in refractive index. Therefore, optical materials, in which one can induce a large change in refractive index by light, are most desirable for holography.

While a number of materials for holography have been developed, polymers functionalized with azobenzene moieties are effective for modulating holograms due to their photosensitivity and reversibility.[1,2] Among these materials, liquid-crystalline polymers (LCPs) containing azobenzene moieties in the side chain are known as high-performance materials for optics due to a large change in birefringence caused by photochemical processes.[3–6] Furthermore, the polymer films have many advantages for practical applications such as stability of optical storage and good mechanical properties.

We previously reported the formation of gratings by means of photochemical phase transition of LCPs containing azobenzene moieties.[7] In general, diffraction efficiency can be improved by inducing a large periodical change in refractive index, which is caused by *trans–cis* photoisomerization of azobenzene molecules,[3–5] followed by a phase transition or an alignment change of LC phases. Furthermore, to obtain a larger change in refractive index in LCPs, we prepared a copolymer of tolane and azobenzene.[8] Tolane derivatives are known as highly birefringent LCs due to their large anisotropy of polarizability.[9] The effect of birefringence (Δn) of LCs on the formation of gratings was studied and the results revealed that a considerable enhancement of η can be achieved in the Raman–Nath regime by using LCs with high birefringence because the change in alignment of mesogens induced by photoisomerization of azobenzene moieties gives rise to the change in birefringence.[8] However, the photosensitivity was not high enough due to the low content of the azobenzene moieties in these LCPs.

To improve the photosensitivity, we prepared LCPs containing both tolane and azobenzene moieties; but unlike conventional LC copolymers, in which azobenzene and tolane are incorporated into their side chains separately, both moieties were attached directly through a central benzene ring and the combined azo-tolane moiety was incorporated into every monomer unit. We also changed the alkyl spacer length between the polymer main chain and the azo-tolane moiety, and explored not only the grating formation behavior of the resulting LCPs but also the photoinduced alignment change of the azo-tolane moiety.

Experimental

Characterization

NMR spectra were recorded in $CDCl_3$ with a Lambda-300. Mass spectra were obtained with a JMS-700 spectrometer with fast atom bombardment (FAB). Molecular weights of the

Chemical Resources Laboratory, Tokyo Institute of Technology, R1-11, 4259 Nagatsuta, Midori-ku, Yokohama 226-8503, Japan.
E-mail: tikeda@res.titech.ac.jp
† Present address: Ebara Research Co., 4-2-1 Honfujisawa 251-8502, Japan.
‡ Present address: Department of Applied Chemistry, Graduate School of Engineering, Hiroshima University, Higashi-Hiroshima 739-8527, Japan.

polymers were determined by gel permeation chromatography (GPC; JASCO DG-980-50; column, Shodex GPC K802 + K803 + K804 + K805; eluent, chloroform) calibrated with standard polystyrenes. LC behavior and phase transition behavior were examined on an Olympus Model BH-2 polarizing microscope equipped with Mettler hot-stage models FP-90 and FP-82. Thermotropic properties of LCPs were determined with a differential scanning calorimeter (Seiko I&E SSC-5200 and DSC220C) at a heating rate of 10 °C min^{-1}. At least three scans were performed for each sample to check reproducibility. The thermodynamic properties and the molecular weights of the LCPs are given in Table 1. Absorption spectra were recorded with a UV-vis absorption spectrometer (JASCO, V-550).

Synthesis of polymers P3AT*m*

The synthesis of monomers **P3AT*m*** is outlined in Scheme 1. **1** and **2** were prepared using a procedure similar to the literature.[10,11] The experimental details are described only for 6-[4-[2-methyl-4-(4-ethoxyphenylethynyl)phenylazo]phenoxy]-hexyl methacrylate (**3AT6**) as an example. **P3AT9** and **P3AT12** were synthesized similarly.

4-(6-Hydroxyhexyloxy)-2′-methyl-4′-(4-ethoxyphenylethynyl)-azobenzene (3)

4-Bromo-2-methyl-4′-(6-hydroxyhexyloxy)azobenzene (**2**) (7.83 g, 20 mmol), 1-ethynyl-4-ethoxybenzene (2.92 g, 20 mmol), $PdCl_2(PPh_3)_2$ (0.70 g, 1.0 mmol), CuI (0.70 g, 3.7 mmol), PPh_3 (1.30 g, 5.0 mmol) were dissolved in triethylamine (20 ml) and THF (20 ml). The mixture was stirred under nitrogen at 60 °C for 8 h. The mixture was cooled to room temperature and extracted with ethyl acetate. After the organic layer was dried with anhydrous magnesium sulfate, the solvent was removed by evaporation. The product was purified by column chromatography (silica gel, ethyl acetate : chloroform = 1 : 1 as eluent) to yield 7.60 g (70%) of orange powder. ^{1}H-NMR ($CDCl_3$, δ/ppm): 1.24–1.63 (m, 6H), 1.41 (t, J = 6.9 Hz, 3H), 1.61–1.83 (m, 2H), 2.67 (s, 3H), 3.66 (t, J = 6.3 Hz, 2H), 4.01–4.05 (m, 4H), 6.86 (d, J = 6.9 Hz, 2H), 6.97 (d, J = 8.1 Hz, 2H), 7.37 (d, J = 6.6 Hz, 1H), 7.46–7.48 (m, 3H), 7.59 (d, J = 8.4 Hz, 1H), 7.89 (d, J = 5.1 Hz, 2H).

6-[4-[2-Methyl-4-(4-ethoxyphenylethynyl)phenylazo]phenoxy]-hexyl methacrylate (3AT6)

A solution of methacryloyl chloride (2.09 g, 20 mmol) in THF (30 ml) was added dropwise at 0 °C to a mixture of **3** (5.00 g, 11 mmol), triethylamine (2.02 g, 20 mmol) and a trace amount of hydroquinone, and the reaction mixture was stirred at room temperature for 24 h. The solution was poured into saturated aqueous sodium hydrogen carbonate, and the product was extracted with ethyl acetate. After the organic layer was dried with anhydrous magnesium sulfate, the solvent was removed by evaporation. The crude solid was purified by column chromatography (silica gel, chloroform as eluent) and finally recrystallized from methanol to yield 3.40 g (68%) of orange solid. ^{1}H-NMR ($CDCl_3$, δ/ppm): 1.39–1.83 (m, 8H), 1.93 (s, 3H), 2.68 (s, 3H), 4.01–4.14 (m, 6H), 5.34 (s, 1H), 6.09 (s, 1H),

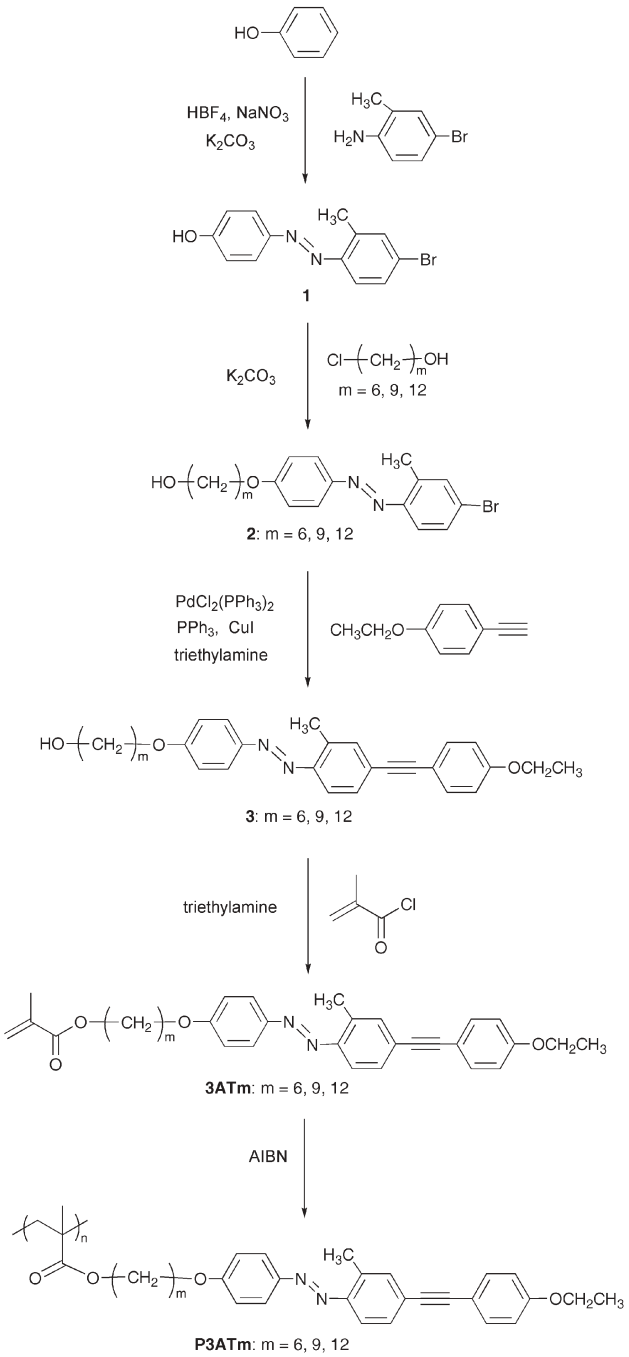

Scheme 1

Table 1 Thermodynamic properties and molecular weights of **P3AT*m***[a]

Polymer	Phase transition temperature/°C	ΔH_{NI}/kJ mol^{-1}	M_n	M_w/M_n
P3AT6	G 47 N 220 I	0.5	23000	1.7
P3AT9	G 39 N 212 I	1.0	21000	3.9
P3AT12	G 34 N 229 I	1.6	34000	3.7

[a] G, glassy; N, nematic; I, isotropic; ΔH_{NI}, change in enthalpy at the N–I phase transition.

6.86 (d, J = 8.4 Hz, 2H), 6.98 (d, J = 8.7 Hz, 2H), 7.37 (d, J = 8.1 Hz, 1H), 7.44–7.47 (m, 3H), 7.59 (d, J = 8.4 Hz, 1H), 7.89 (d, J = 9.0 Hz, 2H). ^{13}C-NMR: 14.66, 17.33, 18.24, 25.70, 28.47, 29.00, 63.41, 64.53, 65.03, 68.03, 88.18, 91.44, 114.45, 114.59, 115.35, 124.81, 125.17, 125.37, 129.49, 133.04, 133.96, 136.39, 137.63, 147.31, 149.80, 159.08, 161.50, 167.40. MS (FAB): 525 (MH^+). Anal. Calcd for $C_{33}H_{36}N_2O_4$: C, 75.54; H, 6.92; N, 5.34. Found: C, 75.78; H, 7.14; N, 5.29%.

Polymerization of monomers 3AT*m*

The experimental procedure for the polymerization of monomer **3AT6** is given below.

3AT6 (0.76 g, 1.4 mmol) and AIBN (3.5 mg, 14 μmol) were dissolved in dry DMF (7.6 ml) and placed in a polymerization tube. After several freeze–pump–thaw cycles, the tube was sealed under high vacuum. Then, the tube was kept at 60 °C for 48 h. The resulting solution was cooled to room temperature and poured into 400 ml of methanol with vigorous stirring to precipitate the polymer. The polymer obtained was purified by repeated reprecipitation from DMF into a large excess of methanol and dried under vacuum for 48 h to yield 0.50 g of **P3AT6** in 66% conversion. ^{1}H-NMR ($CDCl_3$, δ/ppm): 0.88–1.83 (m, 14H), 2.55 (s, 3H), 3.91 (m, 6H), 6.77 (m, 4H), 7.24–7.49 (m, 5H), 7.76 (d, 2H).

Preparation of films

To obtain an oriented film, **P3AT*m*** was dissolved in chloroform, and then a small portion of the resultant solution was cast on a polyimide-coated glass substrate, which had been rubbed to align mesogens. Homogeneously aligned films were obtained after annealing. Thickness of the sample films was measured as 1.2 μm with a surface profiler (Veeco Instruments Inc., Dektak 3ST). This film was used for η measurements. For the investigation of the photoinduced alignment change, the sample films with thickness of about 400 nm were prepared in a similar manner.

Optical setup and measurements

Photoinduced alignment change of LCPs was investigated by the following procedure. The polymer film was irradiated with linearly polarized light at 488 nm from an Ar^+ laser in a glassy state. The direction of polarization of the pumping light was parallel to the aligned direction of mesogens, *i.e.*, *s*-polarization. Intensity of the probe light at 633 nm from a He–Ne laser (NEC, GLC5370, 1 mW) transmitted through a pair of crossed polarizers, with the sample film between them, was measured with a photodiode. The formation of gratings was performed by a procedure similar to the literature.[7] Writing beams were two linearly *s*-polarized beams from an Ar^+ laser. The incident angle of the writing beams was fixed at $\theta = 7°$. In this study, the value of η was defined as the ratio of the intensity of the first-order diffraction beam to that of the transmitted beam through the film in the absence of the writing beams. After grating formation, the surface structure of the LCP films was investigated with an AFM (Shimazu, SPM-9500 J2).

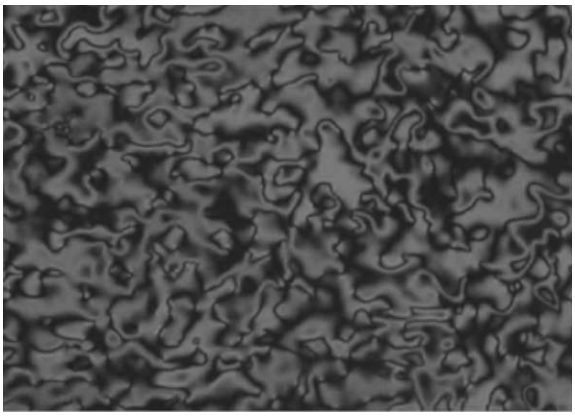

Fig. 1 Polarizing optical micrograph of the texture of **P3AT6** at 200 °C on heating.

Results and discussion

LC behavior of polymers

It was observed with a polarizing microscope that all the polymers used in this study showed an LC phase (Fig. 1). The LCPs exhibited LC states in a broad temperature range (>170 °C) compared with conventional LCPs. We assigned the LC phases of these polymers as nematic phases by POM and DSC measurements. From the DSC curves of **P3AT*m*** (Fig. 2), the phase transition temperature, glass transition temperature (T_g), and the change in enthalpy from the nematic phase to the isotropic phase (ΔH_{NI}) were obtained and are summarized in Table 1. The ΔH_{NI} of **P3AT*m*** increased with the alkyl spacer length. In general, LCPs showing large values of ΔH_{NI} exhibit highly packed states of mesogens. A similar dependence of the ΔH_{NI} on the spacers was already reported by Craig and Imrie.[12]

Change in alignment of LCP

The photoinduced alignment change was brought about in a monodomain state: the direction of alignment of mesogens in a uniaxially aligned LCP film was changed to another direction upon exposure to *s*-polarized actinic light. As shown in Fig. 3, in the initial state (a), the probe light was observed through crossed polarizers, with the sample film between them, because

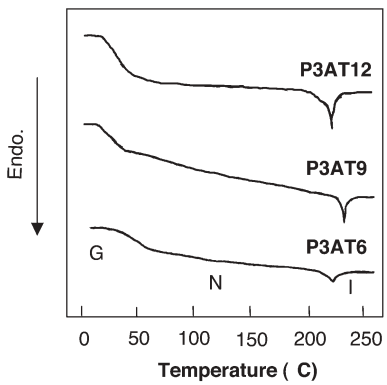

Fig. 2 DSC curves of **P3AT*m*** on the third heating at a rate of 10 °C min^{-1}.

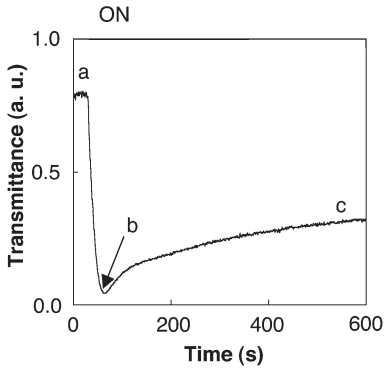

Fig. 3 A typical profile of transmittance as a function of irradiation time in **P3AT6**. The film was exposed to an *s*-polarized beam at 488 nm.

of the birefringence of the LCP. When the film was exposed to the pump beam, the initial order of homogeneously aligned the azo-tolane moieties was destroyed by *trans–cis* isomerization cycles (b in Fig. 3). Upon further irradiation, the transmittance gradually increased and finally became saturated (c in Fig. 3). This result indicates that a change in alignment of azo-tolane moieties is induced photochemically. To discuss the alignment change behavior quantitatively, the order parameter (S) of the LCP was evaluated by using the following equation:

$$S = (A_{//} - A_{\perp})/(A_{//} + 2A_{\perp}) \quad (1)$$

where $A_{//}$ and $A_{\perp}$ are absorbance measured with light polarized parallel and perpendicular to the rubbing direction, respectively. Polarized absorption spectra of the **P3AT6** film measured before and after irradiation with linearly polarized light at 488 nm at room temperature are shown in Fig. 4 where spectra (A), (B) and (C) correspond to the states (a), (b) and (c) in Fig. 3, respectively. Before irradiation, the value of S was 0.41, which indicates a typical aligned nematic LC phase (Fig. 4(A)). In Fig. 4(B), the value of S was 0.11. This value was smaller than that of the initial state because the homogeneously aligned azo-tolane moieties are disorganized by the *trans–cis* isomerization process. In Fig. 4(C), the value of S changed to -0.25, indicating that the alignment of the azo-tolane moieties in **P3AT6** has become perpendicular to the electric vector of the irradiation light. In this study, it has been observed that the transmittance change is caused by the photoinduced alignment change.

Change in birefringence of LCP

Fig. 5 shows the change in transmittance of **P3AT6** at various light intensities. From this result, we evaluated the values of birefringence by using eqn. (2):[13–15]

$$T = \sin^2(\pi d\Delta n/\lambda) \quad (2)$$

where d is the film thickness, Δn is the birefringence of the **P3AT6** film, T is the transmittance, and λ is the wavelength of the probe light (633 nm). In the initial state, the calculated value of birefringence was 0.39. This value is much higher than those of the previous studies,[8] in which two-ring tolane

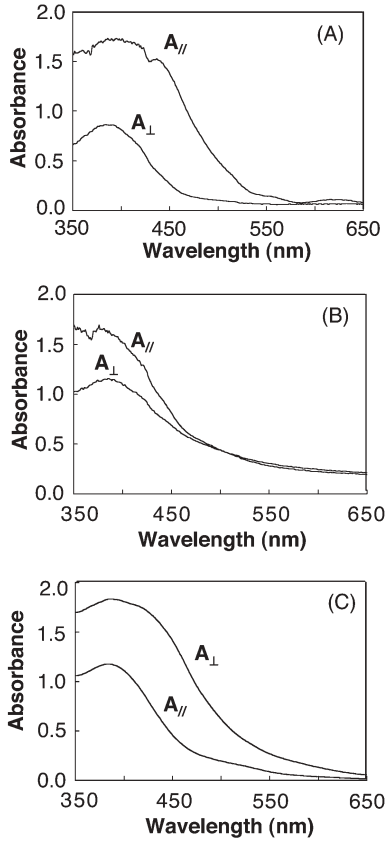

Fig. 4 Polarized absorption spectra of the **P3AT6** film. Spectra (A), (B) and (C) correspond to the states shown in Fig. 3: (A) before irradiation (a in Fig. 3); (B) disruption of the initial order by *trans–cis* photoisomerization (b in Fig. 3); (C) induction of the photoinduced alignment change (c in Fig. 3).

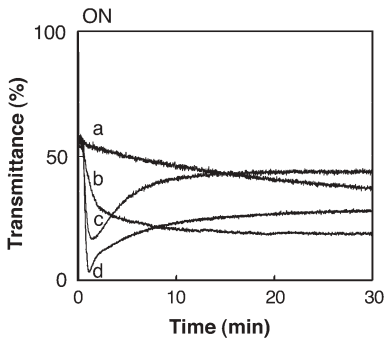

Fig. 5 Change in transmittance of the **P3AT6** film as a function of irradiation time. Films were exposed to an *s*-polarized beam at 488 nm. Light intensity: a, 3 mW cm^{-2}; b, 50 mW cm^{-2}; c, 150 mW cm^{-2}; d, 250 mW cm^{-2}.

moieties are separately incorporated into side chains of LCPs, because azo-tolane moieties could have large anisotropy of polarizability. When the intensity of the pumping beam was 250 mW cm^{-2} and 150 mW cm^{-2}, the transmittance decayed upon irradiation of *s*-polarized light in the glassy state and reached very low values (c and d in Fig. 5). This result indicates that a photoinduced alignment change destroys the initial order of homogeneously aligned azo-tolane moieties and

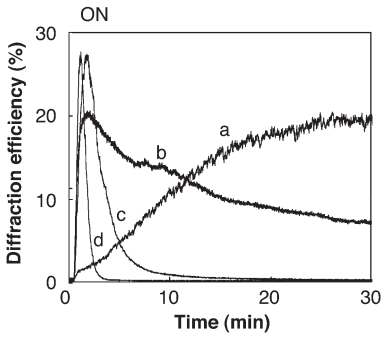

Fig. 6 Change in intensity of diffracted light in the **P3AT6** film as a function of irradiation time. Films were exposed to (s + s)-polarized writing beams at 488 nm. Light intensity: a, 3 mW cm^{-2}; b, 50 mW cm^{-2}; c, 150 mW cm^{-2}; d, 250 mW cm^{-2}.

induces a large change in birefringence ($\approx$0.35). Upon irradiation of the actinic light at 3 mW cm^{-2}, the change in birefringence was 0.15. It was found that one can induce a large change in birefringence in this LCP even though the intensity of the pumping light is several mW cm^{-2}. This observation gives an idea that one can induce a large change in refractive index upon exposure to actinic light if LC materials with high birefringence are employed.

Grating formation in LCP

We attempted the formation of gratings in **P3AT6** at various light intensities (Fig. 6). When the intensity of the writing beams was 250 mW cm^{-2} and 150 mW cm^{-2}, we observed maximum diffraction efficiency (η_{max}) of above 25% within 30 s (c and d in Fig. 6). The rate of the grating formation was much higher than that observed in the previous study.[8] The intensity of the diffracted light increased first with irradiation time, and then it decreased. This behavior could be due to an increase at first, followed by a decrease, of difference in the refractive index between bright and dark areas of the interference patterns. Similar behavior has been reported when high-intensity writing beams were employed.[7] It is worth noting that we observed a value of η of 20% even at writing beam intensity as low as 3 mW cm^{-2}. This result is explicable in terms of the change in transmittance shown in Fig. 5. Namely, a large change in refractive index in the bright areas of the interference patterns is induced even though the change in alignment by light is small. Therefore, it has become apparent that **P3AT6** shows high sensitivity as holographic material. Generally, low-molecular-weight LCs exhibit high sensitivity in the formation of gratings, but possess low stability of stored information.[16,17] However, the LCP film also shows high stability of gratings below the glass transition temperature (T_g).

Modulation of surface structure

Evaluation of photoinduced surface modulation by AFM also demonstrated the formation of gratings. Fig. 7 shows an AFM image which was recorded at a light intensity of 250 mW cm^{-2} for 30 s. After exposure to the writing beams, the η value was about 25%. The formation of surface relief grating (SRG) depends on the polarization configuration of the writing

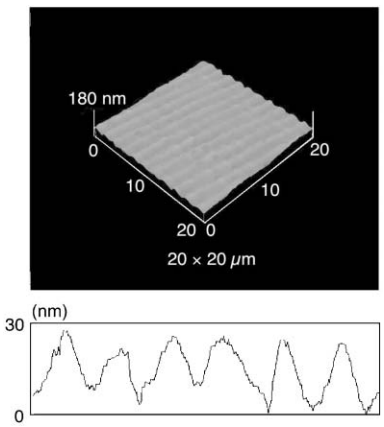

Fig. 7 AFM three-dimensional and slice views of the grating recorded in **P3AT6**. The gratings showed $\eta \approx 25\%$ with a surface modulation of *ca.* 20 nm.

beams. Among them, two s-polarized (s + s) configuration gives rise to a very small surface modulation, nearly negligible (<a few nanometers), and shows the smallest value of η (<0.4%) due to SRG.[18] In this study, we explored the surface modulation of the **P3AT6** films under the (s + s) configuration. Since the periodic structure of the surface relief was about 2.0 μm wide in each case while its height was about 20 nm, the contribution of the surface modulation to the spatial change in refractive index is almost negligible in this study. So we conclude that the gratings are formed by the change in refractive index caused by an order–disorder change of the azo-tolane moieties. From this result, the difference in refractive index between the bright and the dark areas ($\Delta n'$) could be evaluated by eqn. (3):[19]

$$\eta = (\pi d \Delta n'/\lambda)^2 \quad (3)$$

where d and λ are the film thickness and the wavelength of the reading beam, respectively. The maximum value of $\Delta n'$ was estimated as 0.09.

Mechanism for formation of gratings

We explored the relation between the diffracted light intensity and the photoinduced alignment behavior. Fig. 8 shows the dynamics of the change in transmittance by the alignment change as well as the diffraction efficiency of the **P3AT6** film. As is apparent from the change in the diffraction efficiency and the transmittance, the value of η showed a maximum when the transmittance of probe light was minimum. This result indicates that when the destruction of the initial order of the azo-tolane moieties is completed in the bright areas of the interference patterns, the value of η shows a maximum since the difference in refractive index between the bright and the dark areas reaches a maximum (Fig. 9(A)). Upon further irradiation, the value of η gradually decreases due to the order–disorder change of azo-tolane moieties in the dark areas (Fig. 9(B)), which leads to a smaller difference in refractive index between the bright and dark areas. Similar mechanisms have already been reported when high-intensity writing beams were employed.[7]

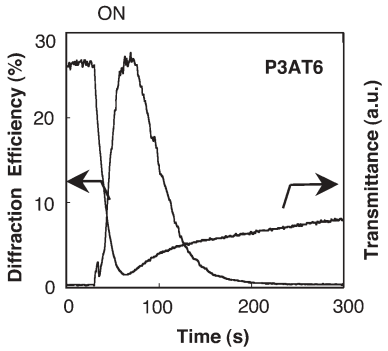

Fig. 8 Typical profiles of the grating formation and the photochemical alignment change in the **P3AT6** film. The intensity of the writing beams and the pumping beam was adjusted to 250 mW cm^{-2}.

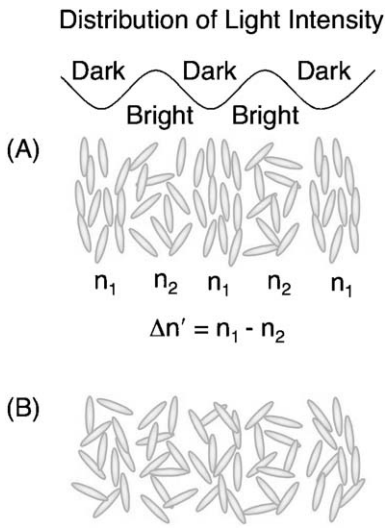

Fig. 9 Plausible mechanism for the formation of gratings in the **P3AT6** film: (A) generation and growth of the modulation of the refractive index in the bright areas in the interference pattern; (B) induction of the photochemical alignment change in the dark areas.

Effect of spacer length on grating formation

The effect of the spacer length of **P3AT*m*** on the diffraction efficiency was evaluated (Fig. 10). We observed a tendency that the formation of gratings takes place faster in the LCPs having shorter alkyl spacers (**P3AT6** > **P3AT9** > **P3AT12**). This tendency could be attributed to the packing density of the azo-tolane moieties because the grating is formed by the order–disorder change of the azo-tolane moieties. Thus the least ordered azo-tolane moieties are likely to be influenced by an external stimulus causing an order–disorder change. It may be assumed that LCPs with low-packing density exhibit high ability to undergo the order–disorder change. From the packing density of the azo-tolane moieties evaluated by ΔH_{NI} (Table 1), **P3AT12** with the largest value of ΔH_{NI} shows the highest resistance to the stimuli that could destroy the ordered structure. The mobility of the azo-tolanes in the LCPs is correlated to the stability of the order of the monodomain state.

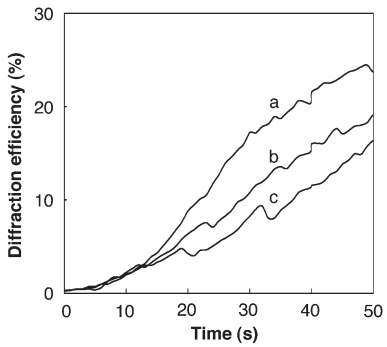

Fig. 10 Change in intensity of diffracted light as a function of irradiation time for the **P3AT*m*** films. a, **P3AT6**; b, **P3AT9**, c, **P3AT12**. Films were exposed to (s + s)-polarized writing beams (488 nm) at 150 mW cm^{-2}.

Conclusion

In summary, we synthesized highly birefringent LCPs containing an azobenzene group directly connected with a tolane moiety. One can induce a large change in birefringence ($\approx$0.35) in three LCPs by the photochemical alignment change. The grating formation in these LCPs could be attributed to the photoinduced order–disorder change of the azo-tolane moieties. The formation of gratings takes place faster in the LCPs having shorter alkyl spacers because the alignment change in the LCPs possessing short spacer length could be easily generated by the order–disorder change. Furthermore the LCP films exhibited high sensitivity as holographic materials. Therefore it might be possible to use these LCPs in compact optical systems.

References

1 T. Todorov, L. Nikolva and N. Tomova, *Appl. Opt.*, 1984, **23**, 4588.
2 A. Natansohn and P. Rochon, *Chem. Rev.*, 2002, **102**, 4139.
3 T. Ikeda and O. Tsutsumi, *Science*, 1995, **268**, 1873.
4 A. Shishido, O. Tsutsumi, A. Kanazawa, T. Shiono, T. Ikeda and N. Tamai, *J. Am. Chem. Soc.*, 1997, **119**, 7791.
5 T. Ikeda, *J. Mater. Chem.*, 2003, **13**, 2037.
6 (*a*) Y. Wu, Y. Demachi, O. Tsutsumi, A. Kanazawa, T. Shiono and T. Ikeda, *Macromolecules*, 1998, **31**, 349; (*b*) Y. Wu, Y. Demachi, O. Tsutsumi, A. Kanazawa, T. Shiono and T. Ikeda, *Macromolecules*, 1998, **31**, 1104; (*c*) Y. Wu, Y. Demachi, O. Tsutsumi, A. Kanazawa, T. Shiono and T. Ikeda, *Macromolecules*, 1999, **32**, 3951.
7 (*a*) T. Yamamoto, M. Hasegawa, A. Kanazawa, T. Shiono and T. Ikeda, *J. Phys. Chem. B*, 1999, **103**, 9873; (*b*) T. Yamamoto, M. Hasegawa, A. Kanazawa and T. Ikeda, *J. Mater. Chem.*, 2000, **10**, 337; (*c*) T. Yamamoto, A. Ohashi, S. Yoneyama, M. Hasegawa, O. Tsutsumi, A. Kanazawa, T. Shiono and T. Ikeda, *J. Phys. Chem. B*, 2001, **105**, 2308; (*d*) M. Hasegawa, T. Yamamoto, A. Kanazawa, T. Shiono and T. Ikeda, *Adv. Mater.*, 1999, **11**, 675; (*e*) M. Hasegawa, T. Yamamoto, A. Kanazawa, T. Shiono and T. Ikeda, *Chem. Mater.*, 1999, **11**, 2764.
8 S. Yoneyama, T. Yamamoto, O. Tsutsumi, A. Kanazawa, T. Shiono and T. Ikeda, *Macromolecules*, 2002, **35**, 8751.
9 (*a*) C. Sekine, K. Iwakura, N. Konya, M. Minami and K. Fujisawa, *Liq. Cryst.*, 2001, **28**, 1375; (*b*) C. Sekine, K. Iwakura, N. Konya, M. Minami and K. Fujisawa, *Liq. Cryst.*, 2001, **28**, 1361; (*c*) C. Sekine, K. Iwakura, N. Konya, M. Minami and K. Fujisawa, *Liq. Cryst.*, 2002, **29**, 355.
10 V. P. Shibaev, S. G. Kostromin and N. A. Plate, *Eur. Polym. J.*, 1982, **18**, 651.

11 A. S. Angeloni, D. Caretti, C. Carlini, E. Chiellini, G. Galli, A. Altomare and R. Solaro, *Liq. Cryst.*, 1989, **4**, 513.
12 A. A. Craig and C. T. Imrie, *Macromolecules*, 1999, **32**, 6215.
13 S. J. Zilker, T. Beiringer, D. Haarner, R. S. Stein, J. W. Egmond and S. G. Kostromine, *Adv. Mater.*, 1998, **10**, 855.
14 A. Stracke, J. H. Wendorff, J. Mahler and G. Rafler, *Macromolecules*, 2000, **33**, 2605.
15 T. Todorov, L. Nikolova and N. Tomova, *Appl. Opt.*, 1984, **23**, 4309.
16 G. P. Wiederrecht and M. R. Wasielewski, *J. Am. Chem. Soc.*, 1998, **120**, 3231.
17 H. Ono and N. Kawatsuki, *Jpn. J. Appl. Phys.*, 1997, **36**, 6444.
18 F. Lagugné Labarthet, T. Buffeteau and C. Sourisseau, *J. Phys. Chem. B*, 1999, **103**, 6690.
19 H. J. Hicher, P. Cunther and D. W. Pohl, *Laser Induced Dynamic Grating*, Springer-Verlag, Berlin, 1986.